Cell Cycle 12:17, 2817–2828; September 1, 2013; © 2013 Landes Bioscience

ZNF365 promotes stalled replication forks recovery to maintain genome stability

Yuqing Zhang[1], Eunmi Park[2], Christopher S Kim[1], and Ji-hye Paik[1,*]

[1]Department of Pathology and Laboratory Medicine; Weill Cornell Medical College; New York, NY USA;
[2]Department of Pediatric Oncology; Dana-Farber Cancer Institute; Boston, MA USA

Keywords: ZNF365, replication stress, cell cycle, PARP1, genomic instability

Abbreviations: DSBs, DNA double-strand breaks; HU, hydroxyurea; BrdU, Bromodeoxyuridine; HR, homologous recombination; NHEJ, non-homologous end joining; CFS, common fragile sites; PARsylated, poly-ADP ribosylated; PBZ, PAR-binding zinc finger domain; PARPi, PARP inhibitors; CPT, camptothecin; TNBC, triple negative breast cancer

The ZNF365 locus is associated with breast cancer risk in carriers of mutated BRCA1 and BRCA2, which are important molecules required for DNA damage response. Previously, we demonstrated that ZNF365 is necessary for timely resolution of replication intermediates of genomic fragile sites and, thus, for suppression of genomic instability; however, the mechanism underlying the function of ZNF365 on damaged DNA and stalled replication forks remains unknown. Here, we demonstrate that ZNF365 is induced by DNA double-strand break (DSB) signals, is involved in the homologous recombination (HR) repair pathway, and maintains genome integrity during DNA replication. On the mechanistic level, ZNF365 interacts with poly(ADP-ribose) polymerase (PARP) 1 to tether MRE11 to the DNA end resection site. Loss of ZNF365 results in delayed mitotic progression and exit due to increased replication stress, ultimately leading to cytokinesis failure, re-duplication of centrosomes, and increased aneuploidy. Collectively, these results suggest an HR repair-dependent function of ZNF365 in preventing genomic instability.

Introduction

DNA damage is generated by exogenous factors, such as chemical agents, UV light, or ionizing radiation, and endogenous factors, such as reactive oxygen species and intrinsic DNA replication errors during cell division. Without correction, such lesions can cause persistent DNA damage, lead to cell death, or result in irreversible mutations that lead to tumorigenesis.[1-3] Therefore, DNA damage repair pathways and the subsequent cellular responses are of vital importance in cancer and age-related disease prevention and treatment. Indeed, individuals with an inherited defect in the DNA repair system are often at an increased risk of cancer.[4,5] DNA double-strand breaks (DSBs) are the most detrimental form of DNA damage and can result in problems for transcription, replication, and chromosome segregation and eventually lead to apoptosis or carcinogenesis. To combat DSBs, cells employ 2 major repair pathways: non-homologous end-joining (NHEJ) and homologous recombination (HR). NHEJ is an error-prone mechanism in which previously unlinked DNA ends are randomly joined without a homologous template. NHEJ, however, is the only DSB repair pathway that is functional in the G_1 phase and can also occur throughout the cell cycle. HR, on the other hand, repairs DSB using the homologous chromosome as a template, resulting in error-free repair. This type of repair occurs primarily during the S and G_2 phases of the cell cycle.[6-8]

The role of replication checkpoints and DNA repair is to ensure proper replication of the genome by removing the underlying causes of replication blockage. DNA replication forks are stalled by DNA lesions, which activate checkpoint proteins such as the ataxia telangiectasia and Rad3-related (ATR). Replication stress-activated ATR promotes replication fork stabilization and DNA repair. Stalled forks restart following HR-mediated repair of DSBs. Proteins involved in this response (i.e., BRCA1, FANCD2, SMC1, HUS1, CHK1) maintain the stability of difficult to replicate genomic regions known as common fragile sites (CFS).[9-11] Hereditary defects in the components of HR-mediated DNA repair pathway or the presence of the mutator phenotype, as exemplified in *WRN*, *BLM*, and *BRCA1/2* mutant patients, cause genomic breakage at fragile sites and lead to both chromosomal rearrangement and genomic instability.[12,13] Loss of function of breast cancer suppressor gene *BRCA2* results in defective HR and triggers genomic instability, thereby accelerating breast cancer tumorigenesis. BRCA2 prevents nucleolytic

*Correspondence to: Ji-hye Paik; Email: jep2025@med.cornell.edu
Submitted: 05/31/2013; Revised: 07/24/2013; Accepted: 07/24/2013
http://dx.doi.org/10.4161/cc.25882

lesions at stalled replication forks by stabilizing RAD51 filaments to maintain genomic integrity through proficient replication fork function.[14] Both the BRCA2 and poly ADP-ribose polymerase (PARP) proteins function in protecting stalled replication forks, and PARP1 activity is required to protect stalled forks from MRE11-dependent degradation.[15] Recent studies have elucidated the mechanism of the monotherapy response to PARP inhibitors (PARPi) in BRCA-mutant, HR-defective tumors. This response stems from increased replication fork stalling with the lack of both HR and PARP1-mediated repair, while increased NHEJ-mediated recombination instigates genomic instability and a proliferation defect.[16-18]

Previously, we identified ZNF365 as a transcriptional target of p53 in the presence of critically short telomeres, and this factor is a novel player that contributes to genomic stability. Loss of ZNF365 leads to incomplete replication of CFS and telomeres, aberrant sister telomere recombination, and increased aneuploidy.[19] Furthermore, ZNF365 expression is downregulated in triple-negative breast cancer (TNBC), and this finding is in line with multiple genome-wide association studies defining ZNF365 as a major breast cancer susceptibility locus in BRCA2-mutant patients.[20,21] Together, ZNF365 may functionally interact with BRCA2 and play an important role in DNA repair pathways. The mechanism of ZNF365 in resolving replication stress is currently unknown. Here, we identified ZNF365 as a necessary component of the HR repair pathway. ZNF365 interacts with PARP1 and tethers MRE11 to the nucleolytic resection sites for replication fork recovery. Loss of ZNF365 resulted in replication stress and induced checkpoint responses that led to delayed mitotic progression, deregulated centrosome dynamics, and, finally, increased genomic instability. Our study demonstrates that ZNF365 is a novel player essential for recovery of stalled replication forks, and that this factor directly contributes to genomic stability.

Results

Loss of ZNF365 contributes to increased DNA damage and correlates with defective HR-mediated DSB resolution

In order to decipher the functional role of ZNF365, we employed ZNF365 transcriptome analysis. Ingenuity pathway analysis of associated gene expression changes in cells with ectopic ZNF365 expression suggested the presence of persistent DNA damage and an overrepresented BRCA-dependent DNA repair pathway (**Fig. S1**). In order to determine the function of ZNF365 in the DNA damage response, we first tested the effect of DSB on the expression of ZNF365. We found that mRNA for *Zfp365* (murine isoform of *ZNF365*) as well as *ZNF365-A* isoform increased 4-fold within 12 h in mouse embryonic fibroblasts (MEFs) and U2OS human osteosarcoma cells following 4 Gy gamma irradiation (**Fig. 1A**). In agreement with these findings, we detected increased protein expression of ZNF365 in both nuclear and cytosolic fractions in response to DSB (**Fig. 1B**). Thus, ZNF365 expression is regulated during the DNA damage response.

Previously, we characterized increased DSB phenotype associated with ZNF365 depletion.[19] In this study, we tested the extent of DSB accumulation in ZNF365-knockdown cells using one of the short hairpins we characterized previously (shZNF-1).[19] Strikingly, lentivirus encoding ZNF365 hairpin-infected U2OS cells exhibited increased 53BP1-positive foci that became more prominent after treatment with the PARP inhibitor ABT-888 (**Fig. S2A**). The effects of ZNF365 depletion on increased DSB foci were consistent in a number of human cell lines (IMR90, Panc-1, MCF7, HCT116, and U87 cells; data not shown), where knockdown of ZNF365 led to an increased basal level of DSB following irradiation or camptothecin (CPT) treatment as demonstrated by the results of an alkaline comet assay (**Fig. 1C**). Because ZNF365-depleted cells exhibit an increased sensitivity to irradiation as well as to DNA damaging agents, we examined the potential role of ZNF365 in the DSB repair pathway. The effect of ZNF365 loss of function on homology-mediated repair was tested in a stable U2OS cell line with a direct repeat GFP (DR-GFP[22]) reporter. Knockdown of ZNF365 suppressed HR-mediated DNA repair (control vs. k.d. = 5.1 vs. 3.1%, $P = 0.04$, **Fig. 1D**). On the other hand, an appreciable increase in the frequency of NHEJ was noted in ZNF365-knockdown cells (control vs. k.d. = 5.6 vs. 6.8%, $P = 0.017$, **Fig. 1E**), and this finding is in agreement with the previously reported counter-balance of the 2 major DSB repair pathways as reviewed by Antoniou et al.[20] These results suggest that ZNF365 is induced by DNA damage signals, and that knockdown cells are defective in the timely resolution of DSB by HR.

Loss of ZNF365 leads to enhanced 53BP1-mediated NHEJ and genomic instability

PARPi have been used successfully to treat BRCA-mutant, HR-defective tumors, because increased replication fork stalling due to the lack of both HR and PARP1-mediated repair provokes genomic instability as well as a proliferation defect.[16,23] Therefore, we examined the effect of PARP inhibition on compromised HR in ZNF365-knockdown cells. ZNF365-depleted cells exhibited dose-dependent sensitivity to the PARP inhibitor ABT-888, and this effect was accompanied by increased 53BP1 foci and frequent radial chromosome formation (Scr vs. shZNF = 48.66 ± 12 vs. 143.5 ± 28.3, $P = 0.0294$, **Fig. 2A**). Of note, recent studies have demonstrated that the embryonic lethality of the $Brca1^{\Delta 11/\Delta 11}$ mouse was reversed by inhibition of 53BP1-mediated repression of DNA resection at the damage sites.[18] Indeed, 53BP1 depletion allows ATM-dependent processing of DNA ends to produce single-stranded DNA, which is required for HR to proceed. We posited that depressed HR and enhanced NHEJ in ZNF365-knockdown cells are also mediated by 53BP1 and together contribute to genomic instability. Therefore, we tested the functional role of 53BP1-mediated NHEJ in increased radial chromosomes formation in ABT-888-treated ZNF365-deficient cells. Tet-inducible hairpins against human or mouse 53BP1 were introduced to knockdown the expression of 53BP1 in U2OS or $Atm^{-/-}$ MEFs,[24,25] respectively (**Fig. S2B**). The frequency of radial chromosomes observed in PARP inhibitor-treated ZNF365-deficient U2OS cells declined with the loss of 53BP1 expression (53BP1+dox vs. –dox = 245.2 vs. 65.6, $P = 0.029$, **Fig. 2A**). Furthermore, the depletion of 53BP1 in ZNF365-knockdown U2OS cells rescued the growth arrest invoked by

ZNF365 knockdown (**Fig. 2B**). In contrast, ZNF365-deficient cells lacking ATM did not recover following 53BP1 knockdown (**Fig. 2C**), supporting a critical role for ATM in restoration of HR as previously reported.[18,26] Collectively, our data suggest that ZNF365 plays a critical role in HR-dependent maintenance of genomic stability, and that deficiency of this factor is compensated by concurrent inactivation of 53BP1, indicating a synthetic survival interaction between these factors.

ZNF365 is necessary for stalled replication fork recovery, and its deficiency leads to mitotic checkpoint activation, multipolar cytokinesis, and aneuploidy

Notably, stalled replication induced by hydroxyurea (HU) caused redistribution of ZNF365 from diffused nucleoplasmic sites to more particulate structures that contained replication protein A (RPA) as well as increased ZNF365 protein expression (**Fig. 2D and E**), demonstrating that the localization and

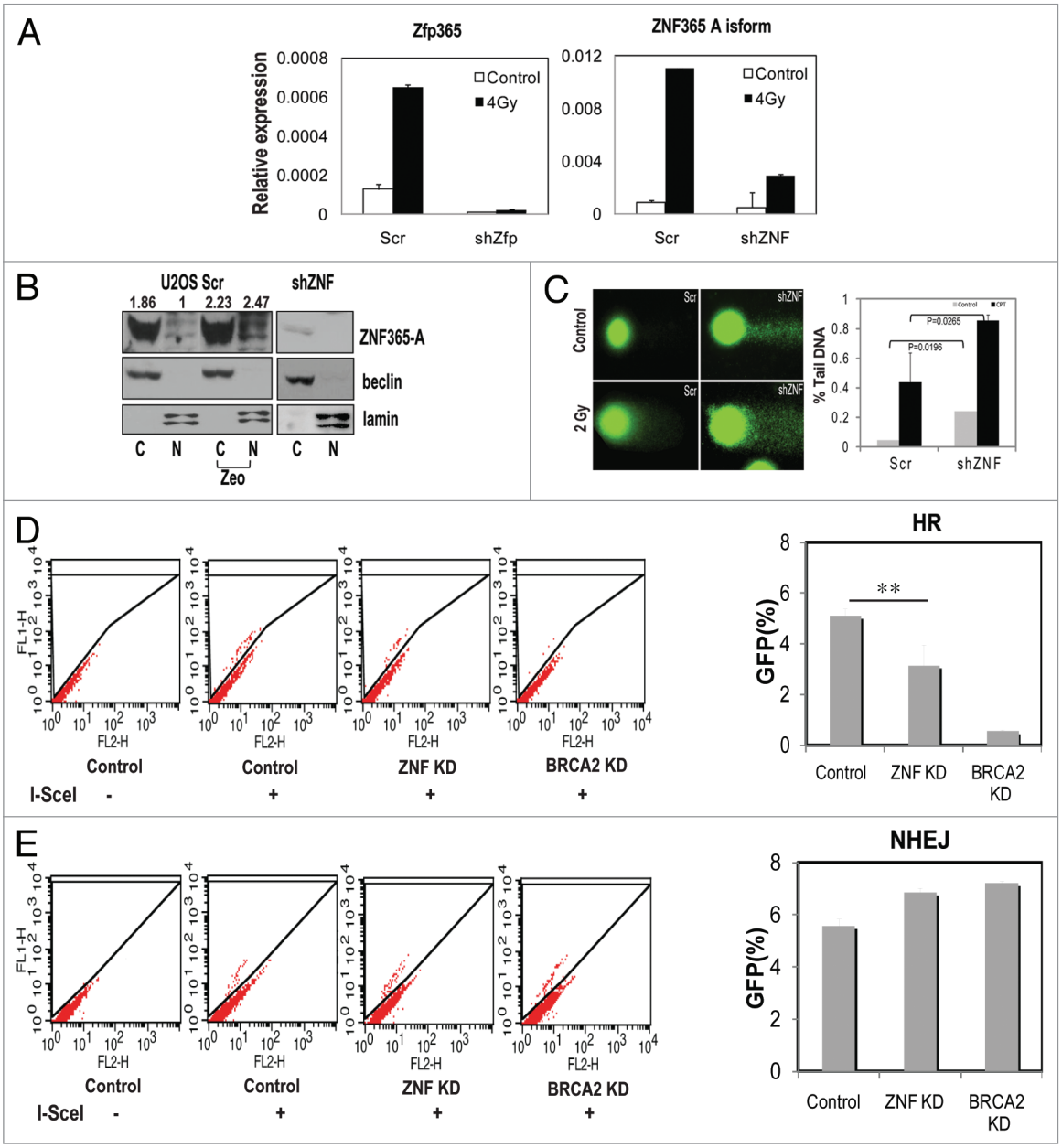

Figure 1. ZNF365 is induced by irradiation, and its depletion correlates with increased DNA damage and defective HR-mediated DSB resolution. (**A**) ZNF365 expression was induced by irradiation. *Atm*$^{-/-}$ MEFs, U2OS Scr, and shZfp or shZNF cells were γ-irradiated. The mRNA levels for ZNF365 were normalized with β-actin. n = 3 (**B**) ZNF365 expression was induced by 12 h zeocin treatment (40 μg/ml). U2OS Scr and shZNF cells were fractionated and analyzed by immunoblot. Beclin and lamin A/C were included as cytoplasmic and nuclear proteins loading controls, respectively. C, cytoplasmic; N, nuclear. Quantified results of ZNF365 expression normalized to loading controls were listed on top. (**C**) ZNF365 protected cells against DNA damage. Representative images from a comet assay for U2OS Scr and shZNF cells γ-irradiated with 2 Gy or treated with 1 μM CPT for 30 min. The mean DNA tail percentage was plotted on right. (**D and E**) Knockdown of ZNF365 impaired HR-mediated DNA repair. Analysis of the frequency of HR- (**D**) and NHEJ- (**E**) mediated DNA repair events in U2OS DR-GFP cells transfected with the indicated ZNF365 or BRCA2 siRNAs. Each value corresponds to the percentage of HR- or NHEJ-positive cells relative to total number of cells analyzed and represents the average of three independent experiments. Error bars represent s.d. $^{**}P < 0.05$.

expression of ZNF365 are regulated during replication stress. Increased DSB may reflect failed resolution of stalled replication at these sites. Thus, we investigated the role of ZNF365 in replication fork recovery. First, we tested whether ZNF365 is involved in the recovery of stalled replication forks based on the possibility that increased DSB in ZNF365-knockdown cells is due to the conversion of arrested replication forks. In support of our hypothesis, pulse-labeling with halogenated nucleosides and analysis of DNA fibers showed significantly decreased fork tract length in the ZNF365-depleted cells following HU-mediated replication arrest (**Fig. 3A**). Without replication arrest, a trend toward decreased replication track length was observed, yet the difference was less significant (**Fig. 3B**). Together, these results place ZNF365 at stalled forks, where this factor seemingly promotes resolution and recovery of replication.

Next, we examined the cell cycle changes caused by defective replication fork recovery in ZNF365-deficient cells. These cells exhibited delayed G_2/M transition after replication arrest at the G_1/S boundary, and this finding is consistent with a role for ZNF365 in replication fork recovery (**Fig. 3C**). Stalled replication forks are stabilized by checkpoint machinery until the causes of cell cycle arrest can be removed, and the cell cycle can be resumed.[27] HU-induced phosphorylation of checkpoint kinases ATR, CHK1 (S317/345), and CHK2 (T68) was further increased in ZNF365-deficient cells (**Fig. 3D**). In addition, the frequency of clonogenic survival following HU treatment for

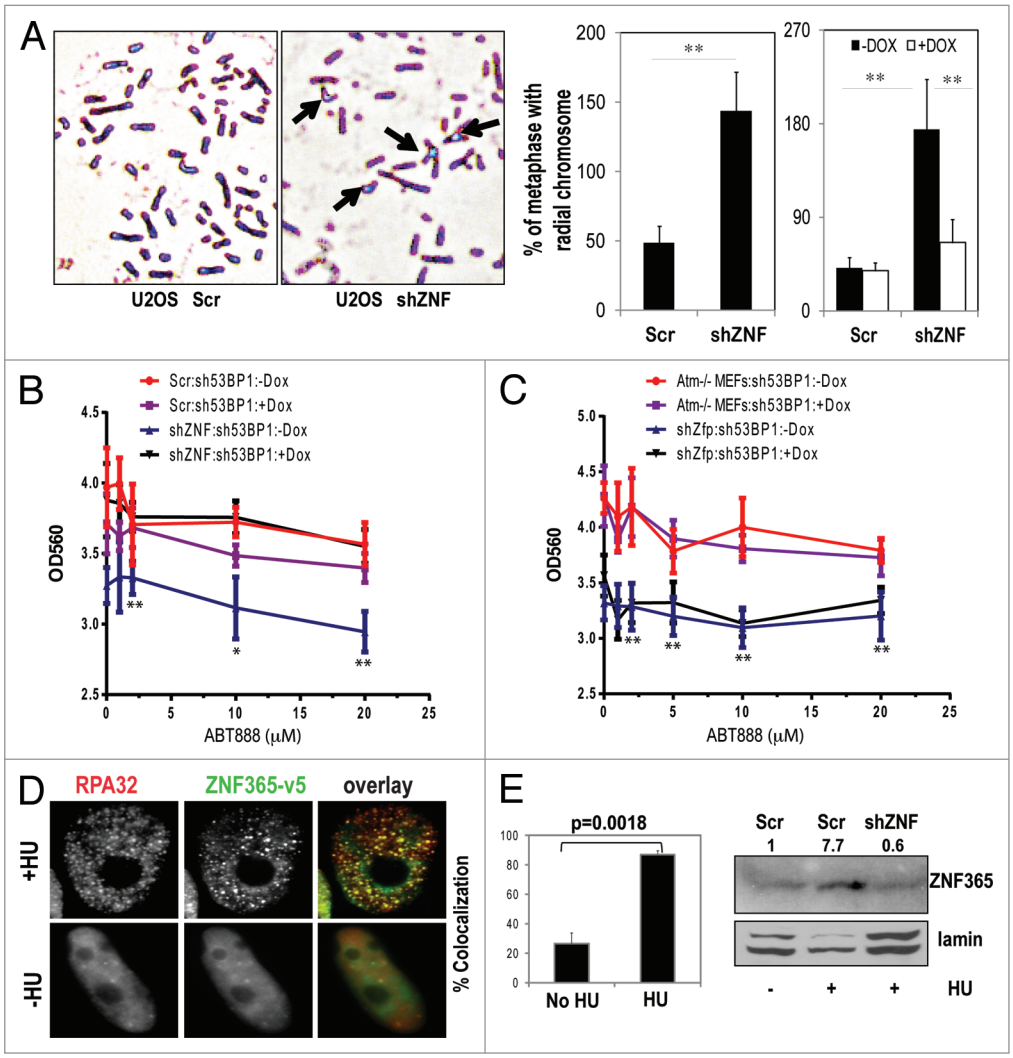

Figure 2. Loss of ZNF365 leads to increased 53BP1-mediated NHEJ. (**A**) Metaphase from U2OS Scr and shZNF cells treated with ABT-888. Arrows pointed to radial chromosome structure. Frequency of metaphase with radial chromosomes was plotted on right side. Quantification of radial chromosome structures upon tet-on knockdown of 53BP1 expression by doxycycline treatment in U2OS Scr or shZNF cells. At least 100 metaphases were counted for each group. $P = 0.0295$ (**B**) Doxycyclin-induced 53BP1 depletion rescued growth arrest by ABT-888 in ZNF365 deficient U2OS cells compared with non-induced cells by MTT assay. Two-way ANOVA was performed to obtain a P value on the cell viability of each group to assess the significance of ABT-888 effect. (**C**) The growth suppression of ZNF365 deficient *Atm*$^{-/-}$ MEFs cells with PARP inhibition could not be reversed by 53BP1 knockdown. * $P < 0.01$, ** $P < 0.05$ (**D**) HU treatment caused re-distribution of ZNF365 into the foci-structure containing RPA. ZNF365-v5 transfected cells were treated with or without 5 mM HU for 24 h and stained with RPA (red) and v5 (green) antibodies. The percentage of colocalization between ZNF365-v5 and RPA foci was plotted on right. (**E**) ZNF365 expression was induced by replication stress. Panc-1 cells were treated with 2 mM HU for 16 h and nuclear fractions were analyzed for expression of ZNF365. The quantified immunoblot result of ZNF365 induction was shown on top.

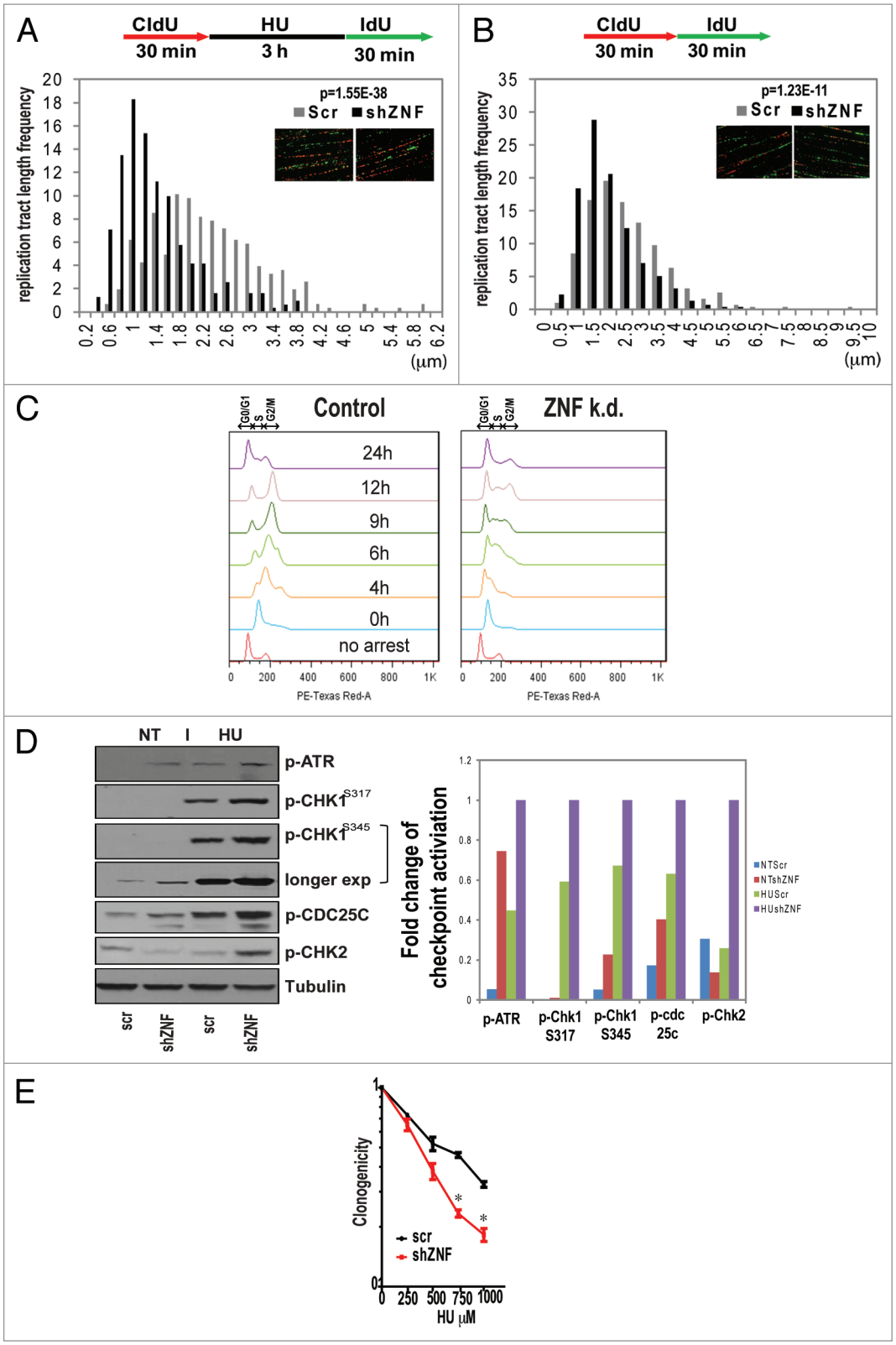

Figure 3. ZNF365 is necessary for stalled replication fork recovery. (**A and B**) Analysis of ongoing replication fork in U2OS Scr or ZNF365 knockdown cells. Top: schematic of the DNA fiber labeling; bottom, ongoing replication fork track length shown as frequency distribution in U2OS Scr and shZNF cells treated with (**A**) or without (**B**) HU for 3 h before the second labeling. The representative images of DNA fibers were shown as insets. (**C**) U2OS cells transfected with or without ZNF365 siRNA were synchronized with HU and then released. At indicated time points cell cycle distribution was analyzed by flow cytometry. (**D**) Depletion of ZNF365 activated checkpoints. U2OS Scr and shZNF cells were treated with 2 mM HU for 3 h and analyzed by immunoblot. Normalized densitometry values were plotted on right. (**E**) Clonogenicity assay. U2OS Scr and shZNF cells were treated with HU for 48 h and released. Viable colonies were stained with crystal violet and scored after 14 d. *$P < 0.05$.

48 h and release was significantly lower in ZNF365-depleted cells (**Fig. 3E**). Together, these results support the notion that replication stress in ZNF365-deficient cells delays cell cycle progression.

We further characterized the molecular events following enhanced replication stress that leads to reduced survival in ZNF365-knockdown cells. Persistent DNA damage signaling and consequent checkpoint activation inhibit mitotic progression by suppressing APC/C E3 ubiquitin ligase activity.[28] Concordantly, phosphorylation of CDC25C, a CHK-dependent G_2/M checkpoint effector, was also significantly increased in ZNF365-depleted cells (**Fig. 3D**). Given the G_2/M checkpoint activation (**Fig. 3D**) and delayed cell cycle progression observed upon ZNF365 knockdown, we hypothesized that inhibition of APC/C activity followed by cytokinesis failure occurred in these ZNF365-depleted cells. In cells that were released following pro-metaphase synchronization, increased inhibitory phosphorylation of CDC2 (CDK1, Y15) and accumulation of APC/C substrates such as Aurora A and B, Cyclin A and B, and Securin, were obvious (**Fig. 4A**). Together, these results point to a role for ZNF365 in effective resolution of replication stress and resumption of the normal cell cycle. Incomplete replication and the ensuing checkpoint response led to delayed mitotic progression and accumulation of mitotic regulators, ultimately contributing to cytokinesis failure.

Interestingly, we noted an abnormal number (>2) of pericentrin- (or gamma tubulin)-positive foci in ZNF365-knockdown cells (**Fig. 4B**). Cultures of these cells exhibited an identical increase in the fraction of cells with more than 4 centrioles (centrin-positive cells), indicating that increased centrosome number is due to duplication of centrioles rather than abnormal fragmentation. Prolonged S-phase arrest by HU treatment uncouples DNA and centrosome replication cycle. We quantitated the fraction of nuclei with an abnormal number of centrosomes after HU-induced arrest in order to distinguish centrosome-autonomous amplification from failed cytokinesis. Typically, only 2–3% of U2OS cells exhibited more than 2 centrosomes when arrested in S phase by HU treatment for 16 h; however, ZNF365-knockdown cells exhibited an additive increase in the frequency of 2 or more centrosome-containing cells rather than a synergistic increase following HU-induced arrest, negating the direct regulation of centrosome duplication (**Fig. 4B**). Finally, knockdown of ZNF365 resulted in 4.9% of cells with supernumerary centrosomes with multipolar mitotic spindles (**Fig. 4C**). After a round of cell division, these cultures accumulated aneuploid cells (**Fig. 4D**). Together, these effects are due to a series of cellular responses: defective nuclear DNA repair induces checkpoint activation and inhibition of mitotic progression and exit, culminating in cytokinesis failure, re-duplication of centrosomes, multipolar cytokinesis, and resultant aneuploidy.

ZNF365 interacts with PARP1 to mediate MRE11-dependent DNA end resection during replication fork recovery

Using mass spectrophotometry analysis of ZNF365 co-immunoprecipitated proteins to identify ZNF365-binding partners, we identified PARP1 as an interacting protein (**Fig. 5A**). Interestingly, both PARP1 expression and overall PARP activity increased upon knockdown of ZNF365, suggesting a potential functional interaction between these 2 factors (**Fig. 5B and C**). Furthermore, ZNF365 co-localized and co-precipitated with PAR polymers following HU treatment (**Fig. 5D**); however, we did not detect PAR modification on ZNF365, suggesting a physical association between ZNF365 and other poly-ADP ribosylated (PARsylated) proteins (data not shown). In addition, co-immunoprecipitation of truncated forms of ZNF365 showed differential binding to PARP1 and MRE11, and both were shown to be PARsylated upon replication stalling.[29] Lack of the C2H2 zinc finger domain in ZNF365 abolished co-precipitation of PARP1 and MRE11, suggesting that the single C2H2 motif may serve as a previously defined PAR-binding zinc finger (PBZ) domain (**Fig. 5E**).[30]

MRE11-mediated nucleolytic resection of DSB is an intermediate step in recovery of stalled replication forks and is followed by RPA coating, RAD51 loading, and homology-mediated strand exchange.[29,31] Previously, PARP1-mediated replication fork restart was shown to be achieved by timely recruitment of MRE11 to the stalled forks through a physical association.[29,32] Notably, ZNF365 and MRE11 co-localized upon HU-mediated replication stalling (**Fig. 5F**). In order to determine whether ZNF365 functions in the nucleolytic resection step, we quantitated the 3′ single-strand generation by MRE11 following induction of DSB. BrdU incorporation is not readily detectable by antibody under native conditions; however, a 3′ single-strand overhang is generated by MRE11 nuclease upon DSB, and BrdU binding within the overhang is detectable without denaturation, serving as an indicator of cellular nucleolytic resection efficiency.[33] Importantly, a clear decrease in resection activity was noted in CPT-treated ZNF365-knockdown cells compared with Scr control cells (**Fig. 5G**). Thus, we hypothesized that impaired recruitment of MRE11 to the replication fork was the cause of this depressed resection activity. Indeed, MRE11 localization to the stalled replication forks was partially impaired in ZNF365-knockdown cells, providing evidence for an intermediate function of ZNF365 between PARP1 activation and nucleolytic resection at stalled forks (**Fig. 5H**). Furthermore, ZNF365 and RAD51 colocalized upon induction of DSB, suggesting that ZNF365 may facilitate RAD51 loading at the HR repair sites (**Fig. S2C**). Together, our results suggest that ZNF365 is necessary for PARP1-mediated replication fork recovery at the end resection step via tethering of MRE11 to the stalled forks.

Discussion

In this study, several lines of evidence support the notion that ZNF365 is a primary responder to stalled replication forks. Inhibition of DNA replication caused increased expression and re-distribution of ZNF365 to stalled replication forks along with single-strand DNA binding protein RPA. Previously, we identified ZNF365 as a component necessary for genomic stability, and demonstrated that its expression was induced by p53 under critically short telomeres. ZNF365 suppressed expression of a subset of CFS, and its loss caused formation of an anaphase ultra-fine DNA bridge, a structure prevalent in Fanconi anemia mutant cells, which harbor a DNA repair-defective cells.[19,34] These

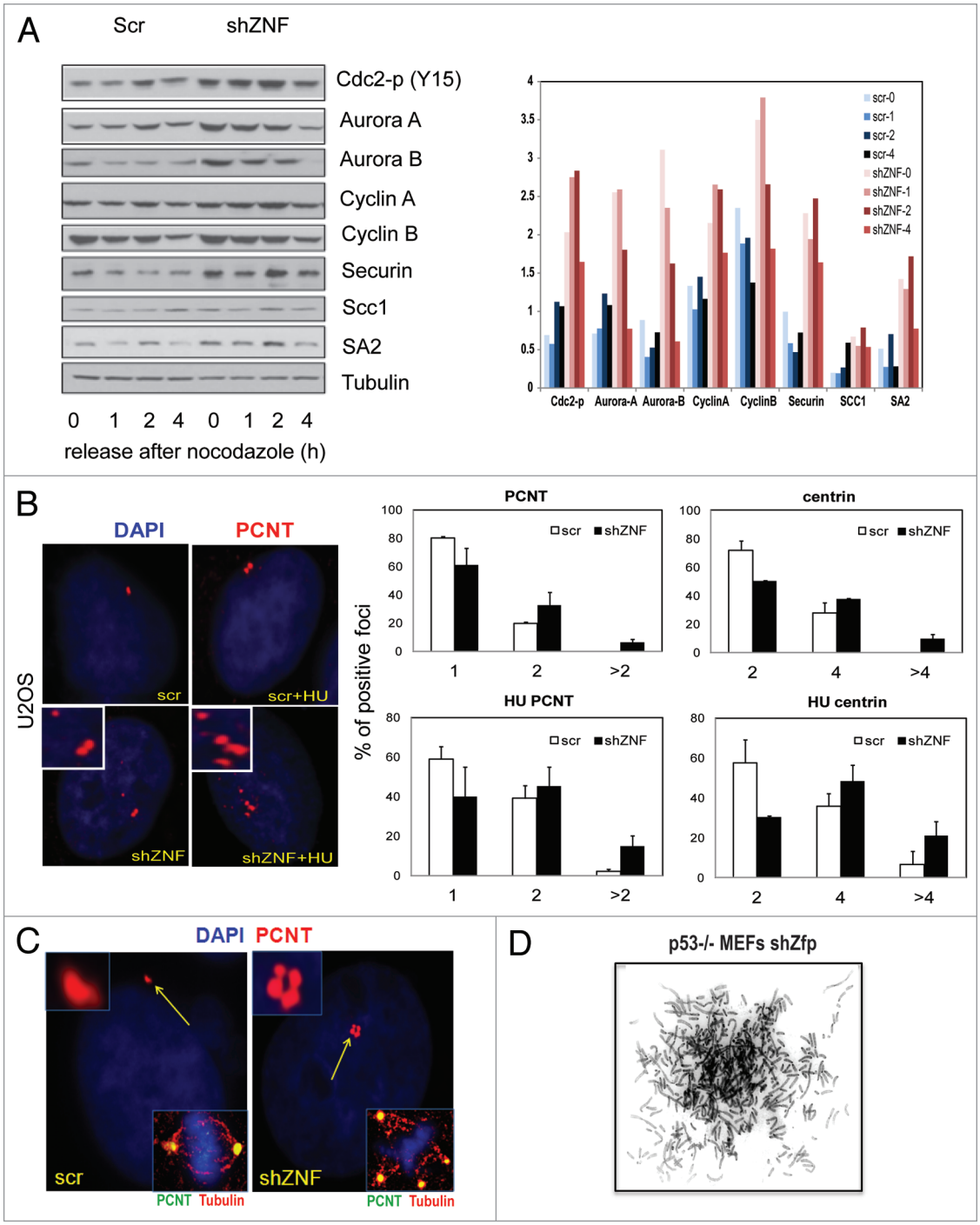

Figure 4. Depletion of ZNF365 leads to mitotic checkpoint activation, multipolar cytokinesis, abnormal centrosome numbers and aneuploidy. (**A**) Delayed mitotic progression in ZNF365-depleted cells. APC/C substrates were stabilized after ZNF365 depletion. Representative immunoblots analysis of U2OS Scr and shZNF cells collected after indicated hours post-nocodazole treatment. Right: quantification of immunoblot band intensity was plotted. (**B**) Knockdown of ZNF365 caused dysregulation of centrosome duplication. PCNT or centrin staining of U2OS Scr and shZNF cells in the presence or absence of 2 mM HU. Insets showed PCNT staining (red) with higher magnification. Centrosome and centriole numbers per cell were plotted on right. Results are shown as mean ± s.d. from multiple experiments. (**C**) Knockdown of ZNF365 caused supernumerary centrosomes along with multipolar spindle formation. Panc-1 Scr and shZNF cells were stained for PCNT (red). Arrows point to centrosomes. Insets showed Panc-1 Scr (bipolar) and shZNF (multipolar) mitotic cells stained for PCNT (green) and α-tubulin (red) with DAPI counterstaining, (**D**) metaphase of *p53*$^{-/-}$ shZfp MEFs exhibiting aneuploidy.

findings are in concert with our new results that demonstrate a role for ZNF365 at the replication fork, where it promotes recovery and resolution of stalled replication.

Our characterization of ZNF365 showed its similarity to previously identified molecules in DNA DSB repair pathways. For example, replication stress-activated ATR and ATM

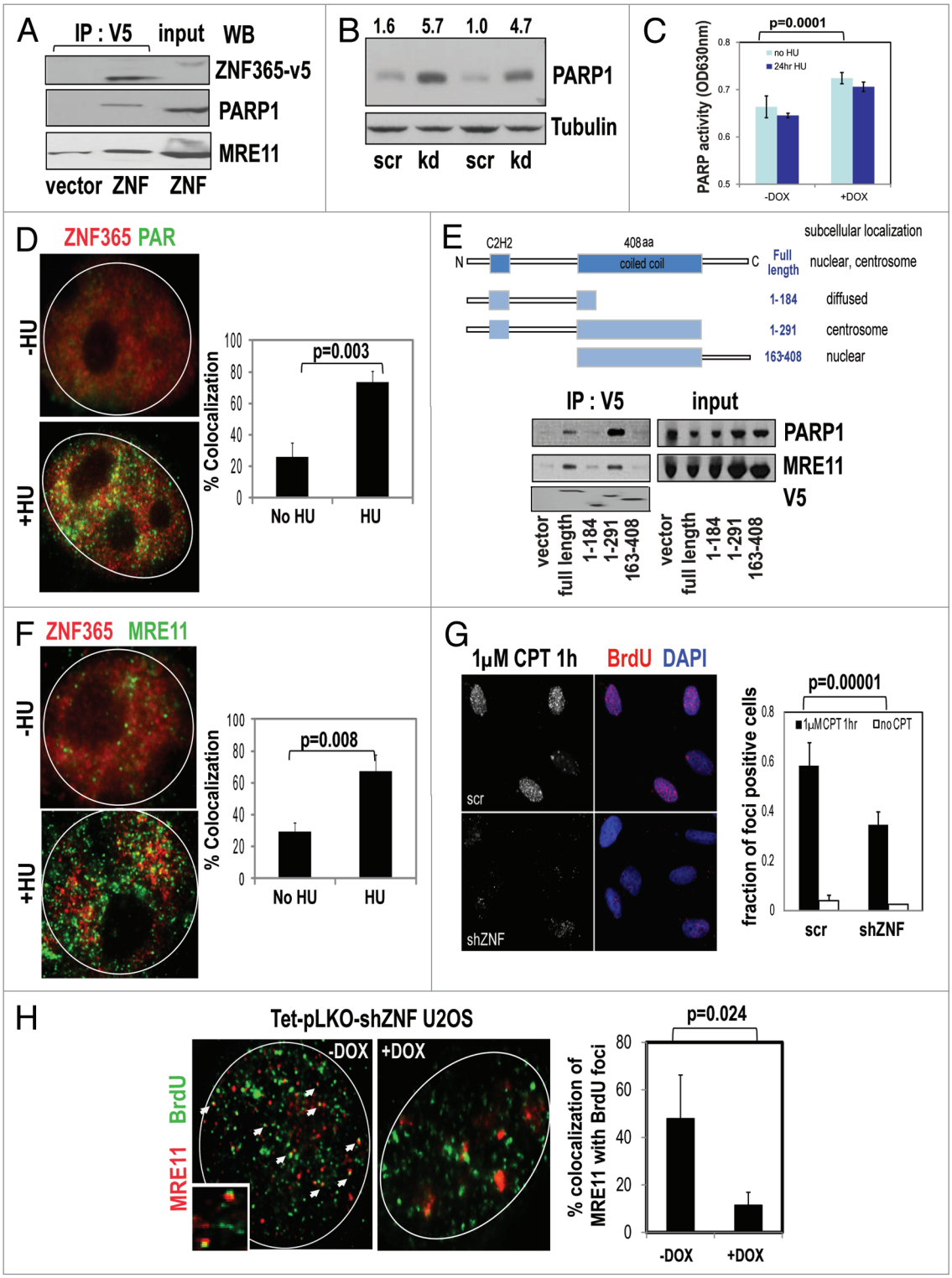

Figure 5. ZNF365 interacts with PARP1 and functions at nucleolytic resection step of fork recovery. (**A**) Co-immunoprecipitation of ZNF365-v5 with PARP1 and MRE11 in 293T cells. Increased expression (**B**) and activity (**C**) of PARP1 upon ZNF365 depletion. (**B**) Quantification of the PARP1 expression after normalization was shown on top. Co-localization of ZNF365 with PAR polymers (**D**) or MRE11 (**F**) following 24 h HU treatment. Cells were treated with HU or not and IF stained for ZNF365-v5, PARsylated proteins, or MRE11. The percent co-localization of ZNF365 with PAR or MRE11 were quantified and plotted on right side. (**E**) Scansite motif prediction of ZNF365 and the constructs and cellular locations of the truncation mutants were shown on top. Co-IP analysis of interaction of ZNF365 truncation mutants with PARP1 and MRE11 (bottom). (**G**) ZNF365 depletion impaired nucleolytic resection steps. BrdU-labeled cells were treated with 1 μM CPT for 30 min and stained for BrdU under a non-denaturing condition. Nuclei with >20 BrdU foci were counted as positive for end resection activity. Data represent the mean ± s.d. (**H**) Tet-on shZNF U2OS cells were pulse-labeled with BrdU followed by HU treatment. Cells were IF stained for BrdU (green) and MRE11 (red). White arrows pointed to co-localization of MRE11 to stalled forks. Percent co-localization of MRE11 with BrdU foci was plotted on right side (n = 8).

phosphorylate WRN helicase to maintain fork integrity and re-establishment of fork progression.[35] Loss of RECQ1 helicase results in replication fork collapse and DNA damage response.[36] Interestingly, RECQ1-deficient cells show defective chromosomal condensation due to untimely DNA replication, reminiscent of anaphase ultra-fine DNA bridges in ZNF365-knockdown cells.[19,36] Our identification of MRE11-dependent DNA end resection as an affected step upon ZNF365 loss supports its role in interplay between HR repair and replication fork recovery. Similarly, DNA2 nuclease mediates replication-coupled repair of DSB at the resection step and interacts with the Faconi anemia interstrand crosslinking (ICL) repair machinery.[37] In agreement, we observed hypersensitivity of ZNF365-deficient cells to a DNA strand crosslinking drug mitomycin C (Park and Paik, unpublished observation). Despite similar phenotypic outcomes upon their loss, the mechanism of action appears to be distinct. We speculate that ZNF365 may function through interacting with other molecules based on its lack of enzymatic activity.

PARP1 is activated at stalled replication forks to recruit DNA repair molecules, and MRE11 is then attracted to stalled forks to promote resection and replication restart.[29] Likewise, the BRCA1/BARD1 heterodimer is recruited to DNA damage sites through the BRCA1 C-terminus (BRCT) motif, which serves as the PAR-binding module.[38] ZNF365 is present in a complex with PARP1 and MRE11, and this interaction requires the N-terminus-containing C2H2 zinc finger motif of ZNF365. This single C2H2 motif may serve as a PBZ domain, which recruits ZNF365 to stalled replication forks or DSB sites. Functionally, a common function of PARP1 and ZNF365 in replication fork recovery is reflected in the altered cell cycle profile observed in their absence. In fact, ZNF365-depleted cells strongly resemble PARP1-null cells, as both cell types have delayed S to G_2/M progression following HU-mediated cell cycle arrest (**Fig. 3C**).[39] In addition, significant upregulation of PARP1 expression and activity in ZNF365-deficient cells suggest compensatory upregulation of a functional partner. Similarly, *BRCA1* mutant tumors overexpress RAD51, which may help to restore defective HR.[40] Additional studies are necessary in order to explore the detailed molecular mechanism of the interaction between PARP1 and ZNF365 in the context of DNA repair response.

PARPi block base excision repair and impair repair of DSB in HR-defective cells, leading to enhanced cytotoxicity.[41] Sensitivity of ZNF365-depleted cells to PARPi in a 53BP1- and ATM-dependent manner predicts its function in the DNA repair pathway. In particular, defects in MRE11 recruitment to the damage sites places ZNF365 in the same pathway with 53BP1-mediated repression of DNA resection. Furthermore, the PARPi sensitivity of ZNF365-depleted *Atm*$^{-/-}$ MEFs was not significantly decreased by 53BP1 knockdown. Thus, this result is consistent with the dependency of nucleolytic resection and HR on ATM activity. Inhibition of PARP combined with chemotherapies that cause DNA damage induces cell death in tumors with defective HR machinery. Cells depleted of ZNF365 exhibited decreased HR, suggesting the potential for therapeutic application of PARPi and ZNF365 targeting in cancer treatment.

Single nucleotide polymorphisms (SNPs) of ZNF365 were identified as a major breast cancer susceptibility loci in BRCA-mutant patients[20,21] by multiple genome-wide association studies. It is possible that these SNPs have other relevant functional links to either BRCA2 and ZNF365 expression or function. As we previously reported, the significantly lowered expression of ZNF365 in TNBC reflects its negative correlation with BRCAness.[19] In the context of decreased BRCA2 function, low expression of ZNF365 may fuel genomic instability, accelerate cancer-promoting mutations, and, thus, facilitate cancer progression. Furthermore, loss of *p53*, the upstream regulator of ZNF365, is an obligatory step in *BRCA1* mutation-associated tumorigenesis, further pointing to multiple mechanisms involved in downregulation of ZNF365.[42,43]

Aneuploidy can be caused by oncogene-induced replication stress, which has been proposed to occur in early neoplastic lesions.[44] Loss of ZNF365 function deregulates centrosome number to further induce chromosomal instability. Multipolar mitosis with the supernumerary centrosomes observed in ZNF365-depleted cells results in cell death or aneuploidy. In yeast, ploidy-mediated lethality was rescued by genes functioning in HR-mediated DNA repair or centrosome regulation, suggesting an important role of these processes in viability of genetically unstable cells.[45] Interestingly, we noted that ZNF365 expression remained high in a number of tumors, including non-TNBC.[19] These results, together, suggest that ZNF365 is likely essential for the viability of cells that develop aneuploidy in light of its function within the HR-mediated repair pathway.

In conclusion, our study suggests that ZNF365 functionally interacts with or promotes the HR repair pathway to facilitate stalled replication fork recovery. These results offer a potential molecular mechanism by which reduced function of ZNF365 instigates genomic instability (**Fig. 6**). Whether ZNF365 functionally contributes to the pathogenesis of breast cancer or other cancers, and whether this factor could be exploited as a biomarker that serves to stratify patients for targeted therapy, warrants future investigation.

Materials and Methods

Antibodies and cell lines

We used rabbit polyclonal antibodies against pATR, pCHK1 (S317 or S345), pCHK2 (T68), pCDC25C (S216), CDC2, Cyclin A, Aurora A, BECLIN, SCC1, SA2, MRE11 (Cell Signaling), pericentrin (Abcam), ZNF365 (Sigma, ab-1), 53BP1 (Bethyl labs), PARP-1, pSMC1 (S957), SMC3 (epitomics). Mouse and rat monoclonal antibodies are including BrdU, Aurora B (Becton Dickinson), BrdU (sheep, Abcam), v5 (invitrogen), α-tubulin (DSHB), RPA32 (cell signaling), lamin A/C (Abcam), and Cyclin B1. U2OS, Panc-1 and IMR90 cells were obtained from the American Type Culture Collection (ATCC). Cells were tested for the absence of mycoplasma and authenticated by standard DNA microsatellite short tandem repeats (PowerPlex 1.2 System, Promega), and the resulting DNA fingerprints were matched to the reference published by ATCC.

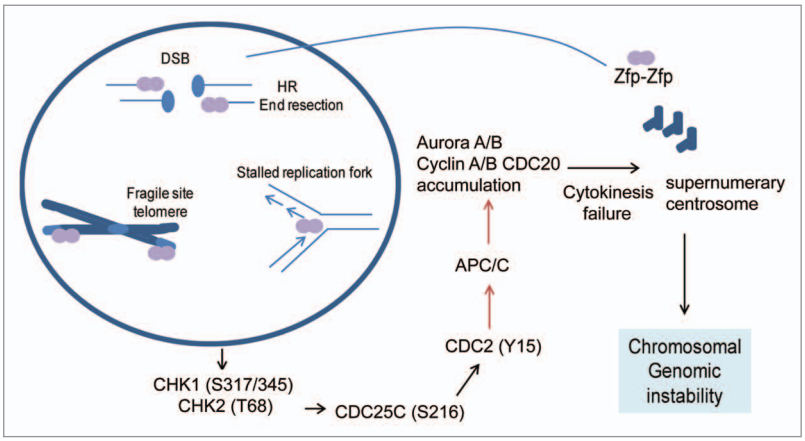

Figure 6. Schematic diagram summary of ZNF365 function. ZNF365 is necessary for HR DSB repair pathway. It binds to PARP1 and tethers MRE11 to the DNA end resection sites for timely resolution of stalled replication forks. Loss of ZNF365 results in incomplete replication and ensuing checkpoint response, leading to delayed mitotic progression and exit, cytokinesis failure, re-duplication of centrosomes, and increased aneuploidy.

Atm$^{-/-}$ MEFs were used to study the effects of ATM effect on the 53BP1 knockdown.

Assay for HR and NHEJ- mediated DSB repair activity

NHEJ and HR assay were performed as previously described.[22] U2OS cells with single-copy incorporation of the NHEJ or DR-GFP reporter were infected with ZNF365 shRNA lentivirus and transfected with I-SceI plasmid. Seventy-two h later, cells were analyzed by flow cytometry. NHEJ or HR activities were determined by the percentage of GFP-positive cells.

DNA fiber analysis

Cells were pulse-labeled with 250 μM IdU after incubation with 25 μM CldU for 30 min. With HU treatment, cells were pretreated with 2 mM HU for 3 h before IdU labeling. Fiber spreads were prepared as described before.[46] Slides were incubated in 2.5 M HCl for 80 min and then washed 3 times in PBS, followed by incubation in blocking buffer (2% BSA in PBS) for 20 min. Primary antibodies 1:250 rat anti-BrdU (detects CldU, AbD seroTec) plus 1:500 mouse anti-BrdU (detects IdU) (Becton Dickinson) were diluted in blocking buffer and incubated for 1 h followed by extensive washes in PBS and secondary antibodies. Pictures were taken from randomly selected fields with untangled fibers and analyzed using the ImageJ software. Minimum of 300 individual fibers were analyzed for each experiment and the mean of at least 3 independent experiments presented. The relative frequency of the red or green replication tracks was scored as a percentage of all the different structures counted. Statistics were calculated using Prism software.

MRE11 colocalization with active replication sites

The sites of active replication in cell were labeled by 15 min incubation with 10 μM BrdU before the HU treatment. After fixing with 4% PFA, cells were detected by immunofluorescence using mouse polyclonal anti-MRE11 (1:100) antibodies, washed with 0.1% Triton in PBS and incubated with goat anti-mouse Alexa Fluor 568-conjugated (1:1000) (Invitrogen) antibodies. Following washing with 0.1% Triton in PBS, cells were incubated in 4% paraformaldehyde for 20 min at room temperature. DNA was denatured for 15 min in 2.5 M HCl, followed by 5 PBS washes and then blocking. The incorporated BrdU was detected with sheep anti-BrdU antibodies and with the goat anti-sheep Alexa Fluor 488-conjugated antibodies according to the standard immunofluorescence procedure.

Co-immunoprecipitation

Cells were lysed with 0.5% NP-40 and 0.5% Triton X-100 lysis buffer containing 50 mM HEPES pH 7.4, 1 mM EGTA, 1 mM $MgCl_2$, 150 mM KCl, 10% glycerol, protease, and phosphatase inhibitors. Four hundred micrograms of protein lysates were incubated with anti-v5 antibody conjugated-beads (Sigma) 4 °C overnight. The beads were washed, boiled in Laemmli's sample buffer and the supernatant was used for SDS-PAGE.

Quantitative RT-PCR

Total RNA was extracted by using trizol RNA extraction protocol. One microgram of total RNA was reverse transcribed into cDNA by using SuperScript® III. Specific primers for qRT-PCR were designed with the primer express 3.0 software (Applied Bisystem). The ZNF365 gene expression was analyzed by real time quantitative PCR using StepOnePlus Real-time PCR system. PCR reaction included the following components: 100 nM each primer, diluted cDNA templates and SYBR Green supermix, and running for 40 cycles at 95 °C for 20 s and 60 °C for 1 min. Each cDNA sample was run as duplicates. The mRNA level of each sample for each gene was normalized to that of the β-actin mRNA. The relative mRNA level was presented as unit values of 2^(Ct[β-actin] – Ct[gene of interest]).

Tetracycline inducible ZNF365 shRNA knockdown

Target sequence within ZNF365 ORF (5′ GAGGAGCTTCTTAGGAAAGAA 3′) was cloned into pLKO-Tet-On lentiviral vector (Addgene). Virus infected cells were selected with puromycin and 1 μg/ml Doxycycline was added for 48 h to induce shRNA expression.

siRNA transfection and cell cycle analysis

One hundred nM ZNF365 siRNA (5′-CATACCAGATTTAGAAGCTTGTCAT-3′, Dharmacon) was transfected into U2OS cells using Lipofectamine 2000. After 24 h, cells were synchronized with 2 mM HU for 16 h and then released. At indicated time points cells were fixed in 70% ethnol, stained with propidium iodide analyzed on BD FACScan. Data were further analyzed with FlowJo software.

Immunofluorescence staining and image analysis

Cells were fixed, permeabilized in 0.2% Trition X-100 followed by staining with different antibodies. All the images of immunofluorescence were acquired by on an Olympus Fluoview confocal microscope using 60× water objective. All data represent the average from at least 3 independent experiments, with at least 100 cells counted per experiment. Significance was calculated using Student 2-tailed *t* test. Differences were considered significant when P was < 0.05.

Clonogenic assay

U2OS Scr or shZNF cells were plated in drug-free medium

at 5 different densities, in triplicates, for the counting of 30–300 clones depending on expected survival. The next day cells were treated with indicated doses of HU (0, 250, 500, 750, and 1000 μM) for 48 h followed by switching to normal growth media. After 14 to 21 d of incubation, colonies were fixed and stained with crystal violet and scored. Only experiments giving a linear correlation between the different dilutions were considered. Cell survival was estimated by dividing the number of colony-forming units in treated samples by the number of colony-forming units in untreated samples, with control cell survival defined as 1.

Statistical analysis

The unpaired two-tail Student *t* test or one-way ANOVA test with Tukey HSD post-test was used to determine significance for all experiments unless noted.

Disclosure of Potential Conflicts of Interest

No potential conflicts of interest were disclosed.

Acknowledgments

J-HP is supported by the Ellison Medical Foundation (AG-NS-0646-10) and the Sidney Kimmel Foundation (SKF-092).

Supplemental Materials

Supplemental materials may be found here:
www.landesbioscience.com/journals/cc/article/25882

References

1. Gupta RC, Lutz WK. Background DNA damage for endogenous and unavoidable exogenous carcinogens: a basis for spontaneous cancer incidence? Mutat Res 1999; 424:1-8; PMID:10232953
2. Mendonca MS, Antoniono RJ, Redpath JL. Delayed heritable damage and epigenetics in radiation-induced neoplastic transformation of human hybrid cells. Radiat Res 1993; 134:209-16; PMID:8488254; http://dx.doi.org/10.2307/3578461
3. Parshad R, Sanford KK, Price FM, Rhim JS, Tarone RE, Fusenig NE, Boukamp P. Association of deficient DNA repair during G2 phase with progression from benign to malignant state in a line of human skin keratinocytes transfected with ras oncogene. Carcinogenesis 1994; 15:33-7; PMID:8293545; http://dx.doi.org/10.1093/carcin/15.1.33
4. Speit G, Trenz K. Chromosomal mutagen sensitivity associated with mutations in BRCA genes. Cytogenet Genome Res 2004; 104:325-32; PMID:15162060; http://dx.doi.org/10.1159/000077511
5. Bouwman P, Jonkers J. The effects of deregulated DNA damage signalling on cancer chemotherapy response and resistance. Nat Rev Cancer 2012; 12:587-98; PMID:22918414; http://dx.doi.org/10.1038/nrc3342
6. Sonoda E, Hochegger H, Saberi A, Taniguchi Y, Takeda S. Differential usage of non-homologous end-joining and homologous recombination in double strand break repair. DNA Repair (Amst) 2006; 5:1021-9; PMID:16807135; http://dx.doi.org/10.1016/j.dnarep.2006.05.022
7. Kim JS, Krasieva TB, Kurumizaka H, Chen DJ, Taylor AM, Yokomori K. Independent and sequential recruitment of NHEJ and HR factors to DNA damage sites in mammalian cells. J Cell Biol 2005; 170:341-7; PMID:16061690; http://dx.doi.org/10.1083/jcb.200411083
8. Brandsma I, Gent DC. Pathway choice in DNA double strand break repair: observations of a balancing act. Genome Integr 2012; 3:9; PMID:23181949; http://dx.doi.org/10.1186/2041-9414-3-9
9. Cha RS, Kleckner N. ATR homolog Mec1 promotes fork progression, thus averting breaks in replication slow zones. Science 2002; 297:602-6; PMID:12142538; http://dx.doi.org/10.1126/science.1071398
10. Casper AM, Nghiem P, Arlt MF, Glover TW. ATR regulates fragile site stability. Cell 2002; 111:779-89; PMID:12526805; http://dx.doi.org/10.1016/S0092-8674(02)01113-3
11. Franchitto A, Pichierri P. Understanding the molecular basis of common fragile sites instability: role of the proteins involved in the recovery of stalled replication forks. Cell Cycle 2011; 10:4039-46; PMID:22101264; http://dx.doi.org/10.4161/cc.10.23.18409
12. Myung K, Datta A, Kolodner RD. Suppression of spontaneous chromosomal rearrangements by S phase checkpoint functions in Saccharomyces cerevisiae. Cell 2001; 104:397-408; PMID:11239397; http://dx.doi.org/10.1016/S0092-8674(01)00227-6
13. Arlt MF, Casper AM, Glover TW. Common fragile sites. Cytogenet Genome Res 2003; 100:92-100; PMID:14526169; http://dx.doi.org/10.1159/000072843
14. Schlacher K, Christ N, Siaud N, Egashira A, Wu H, Jasin M. Double-strand break repair-independent role for BRCA2 in blocking stalled replication fork degradation by MRE11. Cell 2011; 145:529-42; PMID:21565612; http://dx.doi.org/10.1016/j.cell.2011.03.041
15. Ying S, Hamdy FC, Helleday T. Mre11-dependent degradation of stalled DNA replication forks is prevented by BRCA2 and PARP1. Cancer Res 2012; 72:2814-21; PMID:22447567; http://dx.doi.org/10.1158/0008-5472.CAN-11-3417
16. Farmer H, McCabe N, Lord CJ, Tutt AN, Johnson DA, Richardson TB, Santarosa M, Dillon KJ, Hickson I, Knights C, et al. Targeting the DNA repair defect in BRCA mutant cells as a therapeutic strategy. Nature 2005; 434:917-21; PMID:15829967; http://dx.doi.org/10.1038/nature03445
17. Bryant HE, Schultz N, Thomas HD, Parker KM, Flower D, Lopez E, Kyle S, Meuth M, Curtin NJ, Helleday T. Specific killing of BRCA2-deficient tumours with inhibitors of poly(ADP-ribose) polymerase. Nature 2005; 434:913-7; PMID:15829966; http://dx.doi.org/10.1038/nature03443
18. Bunting SF, Callén E, Wong N, Chen HT, Polato F, Gunn A, Bothmer A, Feldhahn N, Fernandez-Capetillo O, Cao L, et al. 53BP1 inhibits homologous recombination in Brca1-deficient cells by blocking resection of DNA breaks. Cell 2010; 141:243-54; PMID:20362325; http://dx.doi.org/10.1016/j.cell.2010.03.012
19. Zhang Y, Shin SJ, Liu D, Ivanova E, Foerster F, Ying H, Zheng H, Xiao Y, Chen Z, Protopopov A, et al. ZNF365 Promotes Stability of Fragile Sites and Telomeres. Cancer Discov 2013; 3:798-811; PMID:23776040; http://dx.doi.org/10.1158/2159-8290.CD-12-0536
20. Antoniou AC, Kuchenbaecker KB, Soucy P, Beesley J, Chen X, McGuffog L, Lee A, Barrowdale D, Healey S, Sinilnikova OM, et al.; CIMBA, SWE-BRCA; HEBON; EMBRACE; GEMO Collaborators Study; kConFab Investigators. Common variants at 12p11, 12q24, 9p21, 9q31.2 and in ZNF365 are associated with breast cancer risk for BRCA1 and/or BRCA2 mutation carriers. Breast Cancer Res 2012; 14:R33; PMID:22348646; http://dx.doi.org/10.1186/bcr3121
21. Gaudet MM, Kirchhoff T, Green T, Vijai J, Korn JM, Guiducci C, Segrè AV, McGee K, McGuffog L, Kartsonaki C, et al.; GEMO Study Collaborators; HEBON Study Collaborators; OCGN; kConFab; EMBRACE. Common genetic variants and modification of penetrance of BRCA2-associated breast cancer. PLoS Genet 2010; 6:e1001183; PMID:21060860; http://dx.doi.org/10.1371/journal.pgen.1001183
22. Pierce AJ, Johnson RD, Thompson LH, Jasin M. XRCC3 promotes homology-directed repair of DNA damage in mammalian cells. Genes Dev 1999; 13:2633-8; PMID:10541549; http://dx.doi.org/10.1101/gad.13.20.2633
23. Helleday T, Bryant HE, Schultz N. Poly(ADP-ribose) polymerase (PARP-1) in homologous recombination and as a target for cancer therapy. Cell Cycle 2005; 4:1176-8; PMID:16123586; http://dx.doi.org/10.4161/cc.4.9.2031
24. Wiederschain D, Wee S, Chen L, Loo A, Yang G, Huang A, Chen Y, Caponigro G, Yao YM, Lengauer C, et al. Single-vector inducible lentiviral RNAi system for oncology target validation. Cell Cycle 2009; 8:498-504; PMID:19177017; http://dx.doi.org/10.4161/cc.8.3.7701
25. Wee S, Wiederschain D, Maira SM, Loo A, Miller C, deBeaumont R, Stegmeier F, Yao YM, Lengauer C. PTEN-deficient cancers depend on PIK3CB. Proc Natl Acad Sci U S A 2008; 105:13057-62; PMID:18755892; http://dx.doi.org/10.1073/pnas.0802655105
26. Goodarzi AA, Jeggo P, Lobrich M. The influence of heterochromatin on DNA double strand break repair: Getting the strong, silent type to relax. DNA Repair (Amst) 2010; 9:1273-82; PMID:21036673; http://dx.doi.org/10.1016/j.dnarep.2010.09.013
27. Branzei D, Foiani M. The DNA damage response during DNA replication. Curr Opin Cell Biol 2005; 17:568-75; PMID:16226452; http://dx.doi.org/10.1016/j.ceb.2005.09.003
28. Townsend K, Mason H, Blackford AN, Miller ES, Chapman JR, Sedgwick GG, Barone G, Turnell AS, Stewart GS. Mediator of DNA damage checkpoint 1 (MDC1) regulates mitotic progression. J Biol Chem 2009; 284:33939-48; PMID:19826003; http://dx.doi.org/10.1074/jbc.M109.009191
29. Bryant HE, Petermann E, Schultz N, Jemth AS, Loseva O, Issaeva N, Johansson F, Fernandez S, McGlynn P, Helleday T. PARP is activated at stalled forks to mediate Mre11-dependent replication restart and recombination. EMBO J 2009; 28:2601-15; PMID:19629035; http://dx.doi.org/10.1038/emboj.2009.206
30. Ahel I, Ahel D, Matsusaka T, Clark AJ, Pines J, Boulton SJ, West SC. Poly(ADP-ribose)-binding zinc finger motifs in DNA repair/checkpoint proteins. Nature 2008; 451:81-5; PMID:18172500; http://dx.doi.org/10.1038/nature06420

31. Ira G, Pellicioli A, Balijja A, Wang X, Fiorani S, Carotenuto W, Liberi G, Bressan D, Wan L, Hollingsworth NM, et al. DNA end resection, homologous recombination and DNA damage checkpoint activation require CDK1. Nature 2004; 431:1011-7; PMID:15496928; http://dx.doi.org/10.1038/nature02964
32. Haince JF, McDonald D, Rodrigue A, Déry U, Masson JY, Hendzel MJ, Poirier GG. PARP1-dependent kinetics of recruitment of MRE11 and NBS1 proteins to multiple DNA damage sites. J Biol Chem 2008; 283:1197-208; PMID:18025084; http://dx.doi.org/10.1074/jbc.M706734200
33. Nimonkar AV, Genschel J, Kinoshita E, Polaczek P, Campbell JL, Wyman C, Modrich P, Kowalczykowski SC. BLM-DNA2-RPA-MRN and EXO1-BLM-RPA-MRN constitute two DNA end resection machineries for human DNA break repair. Genes Dev 2011; 25:350-62; PMID:21325134; http://dx.doi.org/10.1101/gad.2003811
34. Vinciguerra P, Godinho SA, Parmar K, Pellman D, D'Andrea AD. Cytokinesis failure occurs in Fanconi anemia pathway-deficient murine and human bone marrow hematopoietic cells. J Clin Invest 2010; 120:3834-42; PMID:20921626; http://dx.doi.org/10.1172/JCI43391
35. Pichierri P, Ammazzalorso F, Bignami M, Franchitto A. The Werner syndrome protein: linking the replication checkpoint response to genome stability. Aging (Albany NY) 2011; 3:311-8; PMID:21389352
36. Popuri V, Croteau DL, Brosh RM Jr., Bohr VA. RECQ1 is required for cellular resistance to replication stress and catalyzes strand exchange on stalled replication fork structures. Cell Cycle 2012; 11:4252-65; PMID:23095637; http://dx.doi.org/10.4161/cc.22581
37. Karanja KK, Cox SW, Duxin JP, Stewart SA, Campbell JL. DNA2 and EXO1 in replication-coupled, homology-directed repair and in the interplay between HDR and the FA/BRCA network. Cell Cycle 2012; 11:3983-96; PMID:22987153; http://dx.doi.org/10.4161/cc.22215
38. Li M, Yu X. Function of BRCA1 in the DNA damage response is mediated by ADP-ribosylation. Cancer Cell 2013; 23:693-704; PMID:23680151; http://dx.doi.org/10.1016/j.ccr.2013.03.025
39. Yang YG, Cortes U, Patnaik S, Jasin M, Wang ZQ. Ablation of PARP-1 does not interfere with the repair of DNA double-strand breaks, but compromises the reactivation of stalled replication forks. Oncogene 2004; 23:3872-82; PMID:15021907; http://dx.doi.org/10.1038/sj.onc.1207491
40. Martin RW, Orelli BJ, Yamazoe M, Minn AJ, Takeda S, Bishop DK. RAD51 up-regulation bypasses BRCA1 function and is a common feature of BRCA1-deficient breast tumors. Cancer Res 2007; 67:9658-65; PMID:17942895; http://dx.doi.org/10.1158/0008-5472.CAN-07-0290
41. Mukhopadhyay A, Elattar A, Cerbinskaite A, Wilkinson SJ, Drew Y, Kyle S, Los G, Hostomsky Z, Edmondson RJ, Curtin NJ. Development of a functional assay for homologous recombination status in primary cultures of epithelial ovarian tumor and correlation with sensitivity to poly(ADP-ribose) polymerase inhibitors. Clin Cancer Res 2010; 16:2344-51; PMID:20371688; http://dx.doi.org/10.1158/1078-0432.CCR-09-2758
42. Holstege H, Joosse SA, van Oostrom CT, Nederlof PM, de Vries A, Jonkers J. High incidence of protein-truncating TP53 mutations in BRCA1-related breast cancer. Cancer Res 2009; 69:3625-33; PMID:19336573; http://dx.doi.org/10.1158/0008-5472.CAN-08-3426
43. Xu X, Wagner KU, Larson D, Weaver Z, Li C, Ried T, Hennighausen L, Wynshaw-Boris A, Deng CX. Conditional mutation of Brca1 in mammary epithelial cells results in blunted ductal morphogenesis and tumour formation. Nat Genet 1999; 22:37-43; PMID:10319859; http://dx.doi.org/10.1038/8743
44. Liu Y, Heilman SA, Illanes D, Sluder G, Chen JJ. p53-independent abrogation of a postmitotic checkpoint contributes to human papillomavirus E6-induced polyploidy. Cancer Res 2007; 67:2603-10; PMID:17363579; http://dx.doi.org/10.1158/0008-5472.CAN-06-3436
45. Storchová Z, Breneman A, Cande J, Dunn J, Burbank K, O'Toole E, Pellman D. Genome-wide genetic analysis of polyploidy in yeast. Nature 2006; 443:541-7; PMID:17024086; http://dx.doi.org/10.1038/nature05178
46. Jackson DA, Pombo A. Replicon clusters are stable units of chromosome structure: evidence that nuclear organization contributes to the efficient activation and propagation of S phase in human cells. J Cell Biol 1998; 140:1285-95; PMID:9508763; http://dx.doi.org/10.1083/jcb.140.6.1285